

Lawrence Berkeley National Laboratory

Recent Work

Title

Assessment of occupant-behavior-based indoor air quality and its impacts on human exposure risk: A case study based on the wildfires in Northern California.

Permalink

<https://escholarship.org/uc/item/4j33p125>

Authors

Luo, Na
Weng, Wenguo
Xu, Xiaoyu
et al.

Publication Date

2019-10-01

DOI

10.1016/j.scitotenv.2019.05.467

Peer reviewed

1Assessment of occupant-behavior-based indoor air quality
2 and its impacts on human exposure risk: A case study
3 based on the wildfires in Northern California

4
5 Na Luo ^{1, 2, 3}, Wenguo Weng ^{1, 2*}, Xiaoyu Xu ^{1, 2}, Tianzhen Hong ³, Ming Fu ⁴,
6 Kaiyu Sun ³

7 ¹ Institute of Public Safety Research, Department of Engineering Physics, Tsinghua
8 University, Beijing, 100084, P.R. China

9 ² Beijing Key Laboratory of City Integrated Emergency Response Science, Tsinghua
10 University, Beijing, 100084, China.

11 ³ Building Technology and Urban Systems Division, Lawrence Berkeley National Laboratory,
12 USA

13 ⁴ Hefei Institute for Public Safety Research, Tsinghua University, Hefei, Anhui Province,
14 320601, China.

15
16**Abstract:** The recent wildfires in California, U.S., have caused not only
17significant losses to human life and property, but also serious environmental
18and health issues. Ambient air pollution from combustion during the fires
19could increase indoor exposure risks to toxic gases and particles, further
20exacerbating respiratory conditions. This work aims at addressing existing
21knowledge gaps in understanding how indoor air quality is affected by
22outdoor air pollutants during wildfires—by taking into account occupant

1^{*}Correspondence and requests for materials should be addressed to Prof. Weng (email:
2wgweng@tsinghua.edu.cn)

23behaviors (e.g., movement, operation of windows and air-conditioning) which
24strongly influence building performance and occupant comfort. A novel
25modeling framework was developed to simulate the indoor exposure risks
26considering the impact of occupant behaviours by integrating building
27energy and occupant behaviour modeling with computational fluid dynamics
28simulation. Occupant behaviors were found to exert significant impacts on
29indoor air flow patterns and pollutant concentrations, based on which,
30certain behaviors are recommended during wildfires. Further, the actual
31respiratory injury level under such outdoor conditions was predicted. The
32modeling framework and the findings enable a deeper understanding of the
33actual health impacts of wildfires, as well as informing strategies for
34mitigating occupant health risk during wildfires.

35

36**Key words:** human exposure risk, indoor air quality, occupant behavior,
37respiratory injury, NAPA wildfire, computational fluid dynamics simulation

38

39Introduction

40Climate change is influencing large wildfire frequency and globally
41widespread disturbance that affect both human and natural systems
42(Hurteau et al. 2014). The 2013 Rim Fire in California has caused an average
43PM_{2.5} concentration of 20 µg/m³ and ranged from 0 to 450 µg/m³, which was
44proved to exert significant adverse health effects to a large population
45(Navarro et al. 2016). As another one of the worst wildfires recently, several
46massive wildfires swept Napa and Sonoma counties in the North Bay areas of
47San Francisco on the western coast of the United States on the night of
48October 8, 2017 (HST). The fires resulted in the worst air quality that has
49ever been recorded in the San Francisco Bay Area¹. The outdoor air quality
50index^{2,3}, measured in particulate matter (e.g., PM_{2.5}) exceeded 250 ug/m³,
51and a measure of other criteria pollutants⁴ (e.g., sulfur dioxide – SO₂)
52exceeded 200 ppb, indicating that the high level of air pollution could cause
53serious health effects in most people who breathed in the contaminated air
54outdoors.

55A sudden increase in the number of hospitalizations during the days
56following the fires could be related to the negative health effects of high
57gaseous and particulate pollutant levels in the area, which included

³¹ Xinhua. Massive wildfires engulf north San Francisco counties.

⁴http://news.xinhuanet.com/english/2017-10/10/c_136667925.htm Accessed 2017-10-10

⁵² EPA USA. Air Data: Air Quality Data Collected at Outdoor Monitors Across the US.

⁶<https://www.epa.gov/outdoor-air-quality-data> Accessed 2018-06-15

⁷³ Air Quality Data Query Tool. <https://www.arb.ca.gov/aqmis2/aqdselect.php> Accessed 2018-806-15

⁹⁴ The criteria pollutants (also known as “criteria air contaminants – CAC”) are a set of air
10pollutants (normally six common pollutants, which are ozone, particulate matter, carbon
11monoxide, lead, sulfur dioxide, and nitrogen dioxide) that cause smog, acid rain and other
12health hazards.

58increased risk for asthma, and deterioration of pre-existing respiratory
59diseases (Lewis et al. 2013). A number of recent researches reported effects
60of the different airborne particle metrics on respiratory diseases,
61cardiovascular effects, lung cancer, asthma, and lung cancer via human
62inhalation exposure (You et al. 2017; Haikerwal et al. 2015; Haddrell et al.
632015). In other words, during the past decades, wildfires have exerted a
64large negative global impact on human health, ecosystems, societies,
65economies and climate(Jolly et al. 2015; Jaffe et al. 2013). Even worse,
66according to the California's Fourth Climate Change Assessment Report
67(Bedsworth et al. 2018), there is no sign of abating in the expansion of
68wildfires due to the climate variations. There is an urgent need to mitigate
69the impacts of the adverse air quality on the human health caused by the
70increasing wildfires (Anderson et al. 2018; West et al. 2013).

71 Since individuals spend an average of 87% of their time indoors (Klepeis et
72al. 2001), indoor air quality (IAQ) is probably more indicative of the pollution
73exposure levels affecting residents' health than the outdoor measures.
74According to the report by the Institute of Medicine (2011), IAQ is affected by
75three main factors: occupant behavior (OB), building characteristics, and
76pollutant properties. Among them, as the most significant factor, OB affects
77IAQ through occupants' interactions with the outdoor physical environment.
78Behaviours such as window opening and closing (Stabile et al. 2017), HVAC
79operation, and walking into or out of a room (Montgomery et al. 2015) will
80change the boundary conditions of the indoor environment, thus influence

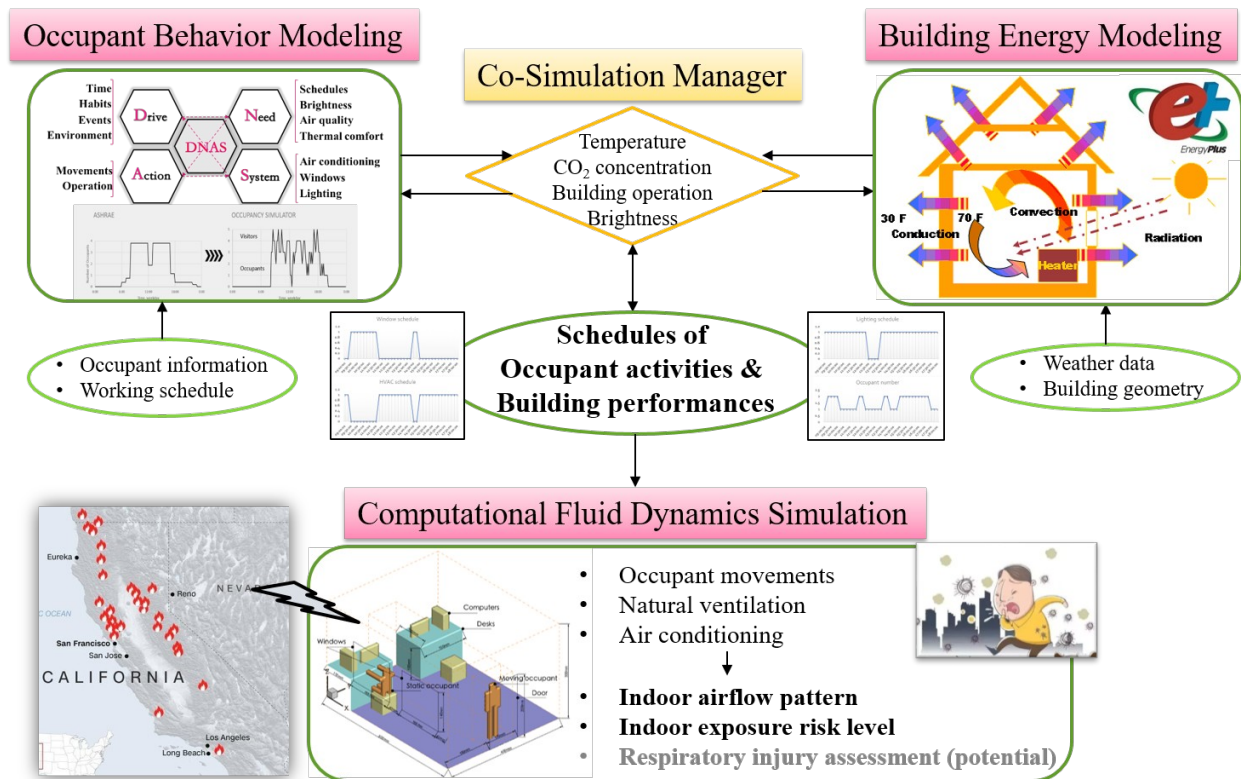
81the flow pattern of indoor air, which, ultimately cause the increase or
82decrease of the indoor pollution levels.

83 Many previous experimental studies focused on the separate impacts of
84occupant behaviors and building performances on the indoor airflow patterns
85and pollutant diffusion process, such as human movements, air-conditioning
86system-related parameters and window operation-related natural ventilation
87(Luo et al. 2016; Luongo et al. 2016). Several Computational Fluid Dynamics
88(CFD) models have also been improved by validating with quantitative
89measurements (Luo et al. 2018b; Gosselin and Chen 2008). These
90investigations revealed detailed information about indoor air flow patterns
91and pollutant concentration levels under different specific conditions.
92However, in a real office environment, occupant behaviors are always
93complex and dynamic due to transient indoor conditions such as
94temperature, humidity, and occupant counts, which are mostly associated
95with the outdoor environment (Lin et al. 2017). Also, when assessing the
96impacts of the indoor environment on human health, exposure to air
97pollution is not only largely determined by pollutant concentrations in the
98spaces where people spend their time, but also by the amount of time they
99spend in those spaces. Therefore, the static status of the indoor environment
100is no longer suitable and appropriate for evaluating the indoor human
101exposure risks during daily working hours; a set of OB-related dynamic
102schedules should be first generated to guide the indoor CFD modeling and
103risk evaluation. Furthermore, for a given indoor environment, the respiratory

injury level is also crucial for assessing adverse health impacts of wildfires, which requires the pollutant concentration near the oro-nasal as the boundary condition for assessment. PM_{2.5} and ultrafine particles are both considered as the representative pollutants when indicating the indoor air quality level to the public (Ibald-Mulli et al. 2002; Zhao et al. 2009). Several studies recognized that PM_{2.5} are better related to resuspension phenomena and combustion processes, while quite a high amount of our overall daily dose of ultrafine particles is due to the indoor sources. Considering the access to the measured data for further validation, we selected PM_{2.5} as the main particle metrics in this work.

Here we used both EnergyPlus and Fluent to co-simulate indoor occupant behaviors as well as the corresponding IAQ and particle deposition inside respiratory systems, respectively. Indoor pollutant concentrations were simulated and used to calculate the IAQ index, which indicated potential adverse health effects. Results of the properties affected by particle concentrations near the mouth and nose of occupants, could be potentially used as the initial and boundary conditions for the assessment of the respiratory injury. Outcomes from the study formulated a framework for modeling (as shown in Figure 1) exposure to indoor pollutants as well as the potential assessment of human health hazards in an office environment—considering occupant movement and behavior, which can inform strategies to mitigate occupant health issues during times of serious outdoor air pollution such as wildfires. For broader application, this co-simulation

framework among Building Energy Modeling (BEM), occupant behavior modeling and CFD builds a bridge in the outdoor-to-indoor penetration process especially considering the indoor occupant behaviors, which thus could be broadly applied in the assessment of indoor quality under many other extreme weather events or use cases such as haze pollution in China, as well as the vehicle exhaust etc.



133

Figure 1 Overview of the modeling framework. The Building Energy Modeling tool (EnergyPlus) was co-simulated with the Occupant Behavior Modeling tool (obFMU - a functional mockup unit of occupant behavior model) to calculate the occupant-related schedules, primarily based on the outdoor environment and the building performance. These modeled activities and building performances were then integrated into the Fluent modeling process as the boundary conditions through a C++ user-defined function (UDF), to further calculate the indoor airflow and contaminant concentration. Eventually, the corresponding indoor exposure risk could be evaluated, as well as the respiratory injury level as one of the potential assessments in the future work.

144

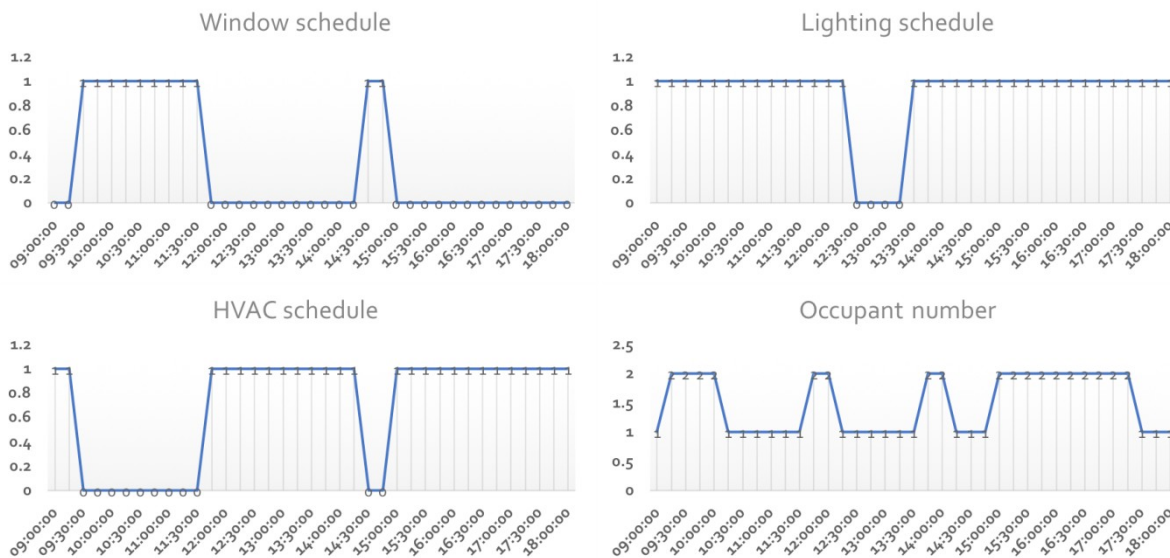
145 **Materials and Methods**

146 **Occupant behavior modeling.** Whole building performance simulation,
147 using EnergyPlus coupled with obFMU, has been used to simulate occupant
148 behavior and generate occupant-related schedules in the last decade (Hong
149 et al. 2017). EnergyPlus is an open-source program that models heating,
150 ventilation, cooling, lighting, water use, renewable energy generation, and
151 other building energy flows (Crawley et al. 2001). It is the flagship building
152 simulation engine supported by the United States Department of Energy
153 (DOE). The occupant behavior function mockup unit (obFMU) is an occupant
154 behavior-modeling tool developed by Lawrence Berkeley National Laboratory
155 (T. Hong et al. 2016). It was developed for co-simulation with EnergyPlus,
156 requiring an XML file generated based on the obXML (occupant behavior
157 eXtensible Markup Language) schema (Hong, D'Oca, Taylor-Lange, et al.
158 2015) and a configuration file. The obXML schema describes the occupant
159 behavior by implementing a DNAS (drivers-needs-actions-systems)
160 framework (Hong, D'Oca, Turner, et al. 2015). The obFMU is the engine for
161 occupant behavior simulation and co-simulates via the functional mockup
162 interface (FMI) with building performance simulation programs, e.g.,
163 EnergyPlus and ESP-r.

164 **Occupant behavior activities.** In this work, the simulated scenario is
165 designed in an office room with two occupants working as different types.
166 One occupant keeps working on the computer, while the other works as a
167 secretary, who might often walk out of the room to get printed materials or

coordinate with other people. The simulation period is from 9:00am to 6:00pm, which are the working hours for the office workers. According to the weather data on October 13, 2017, the building performance, including the four occupant-related schedules and the operation characteristics of the indoor facilities, were modeled in EnergyPlus. Four categories of occupant behavior models were used in this study: occupant movement, lighting, windows, and HVAC operation. They were used to describe the characteristics of related occupant behaviors, based on which the probability of occupants taking an action is estimated. More specifically, Chen's agent-based stochastic occupant movement model (Chen et al. 2018), Haldi's lighting control models (switch on light at arrival or when it is dark, switch off at departure) (Haldi 2013), and Newsham's window control model (open at arrival or when the outdoor environment is suitable, close at arrival, departure or when the outdoor environment is not suitable) (Newsham 1994) were adopted. HVAC operation is a combination of availability schedule and actual window operation. In other words, when the window is open, the HVAC system will be off; when the window is closed, the HVAC system will be on if occupants feel hot. The occupant behavior models were compiled in an obXML file, which worked as the input to obFMU and was used to co-simulate with EnergyPlus. Occupant-related schedules, including the occupancy schedule, lighting schedule, natural ventilation schedule (namely window schedule), as well as the HVAC schedule were generated in the simulation process, seen in Figure 2. As for the detailed characteristics, the operation

191parameters of the windows and HVAC refer to the velocity, temperature, and
 192pollutant concentration of the inlet airflow. The electric power of the lighting
 193and computers was associated with the indoor environment in the modeling
 194process. The changes of occupant count represented the moments when the
 195occupant was entering or leaving the room.



196
 197**Figure 2. Four occupant-related schedules from the co-simulation of**
 198**EnergyPlus and obFMU.**

199**Indoor air flow field modeling.** The CFD software ANSYS Fluent (Version
 20018.0.0) was employed to simulate the transient indoor flow field affected by
 201the occupant behaviors. Gambit (Version 2.4.6) was used to build the
 202geometric model of the office room (Figure 3) and generate the grids for
 203simulation. The total number of grids is 6.7 million. The minimum mesh
 204volume was $2.64 \times 10^{-9} \text{m}^3$, located close to the skin of the moving occupant.
 205The method of mesh generation was used in our previous study (Luo et al.
 2062018a, 2018b). The transient solver was employed during the calculation. As
 207for representing the turbulence airflow caused by the ventilation and

208occupant movements, the RNG k- ϵ model adopted in this work was validated
209by previous work (Zhang et al. 2009; Han et al. 2014; Fracastoro et al. 2002),
210with the overall consideration of accuracy, computing efficiency, and
211affordability for modeling the indoor flow field. The differential viscosity
212model and the swirl dominated flow in the RNG options were selected.
213During the iterative process, the pressure-implicit with splitting of operators
214(PISO) algorithm was employed to solve the pressure-velocity coupling
215equations. The second-order upwind scheme was also used to consider the
216diffusion-convection in the governing equation. The Discrete Element Model
217(DEM) Collision term and the Brownian Motion term were both applied to
218include the particle-particle interactions (voidage and collision), which
219captured the particle resuspension phenomenon of PM_{2.5}. According to the
220aforementioned schedules and the related parameters, a UDF in the Fluent
221software has been created to automate the transient changes of the window
222boundary conditions, HVAC boundary conditions, light conditions, and the
223human movement status. The gaseous composition and the corresponding
224concentrations of the inlet airflow were based on the measured outdoor air
225quality data, seen in Table 1. The time steps during the occupant moving and
226static process were set to 0.01 s and 1 s, respectively. The calculation is
227computed in a four-node Linux cluster. Each node of the cluster has 12
228processors (2.4 GHz Intel 64). The overall simulation period in this case is
229nine hours (32400 seconds), which requires 120 hours of the computing
230time.

Table 1. The daily maximum outdoor air quality of some criteria pollutants (SO₂, CO, and O₃) and the particulate matter (PM_{2.5}) within the following week after the wildfire event in Northern California (October 8 - 14, 2017). The gaseous composition and the corresponding concentrations of the inlet airflow was based on the measured outdoor air quality data.

	Oct. 8	Oct. 9	Oct. 10	Oct. 11	Oct. 12	Oct. 13	Oct. 14
SO ₂ (ppb)	65.90	89.49	/	/	248.93	439.05	345.92
CO (ppm)	0.80	1.19	/	1.29	1.83	2.84	2.29
O ₃ (ppb)	12.72	25.49	31.40	33.54	76.57	92.08	50.48
PM _{2.5} (ug/m ³)	86.30	115.3	214.70	/	91.97	212.49	179.40

0

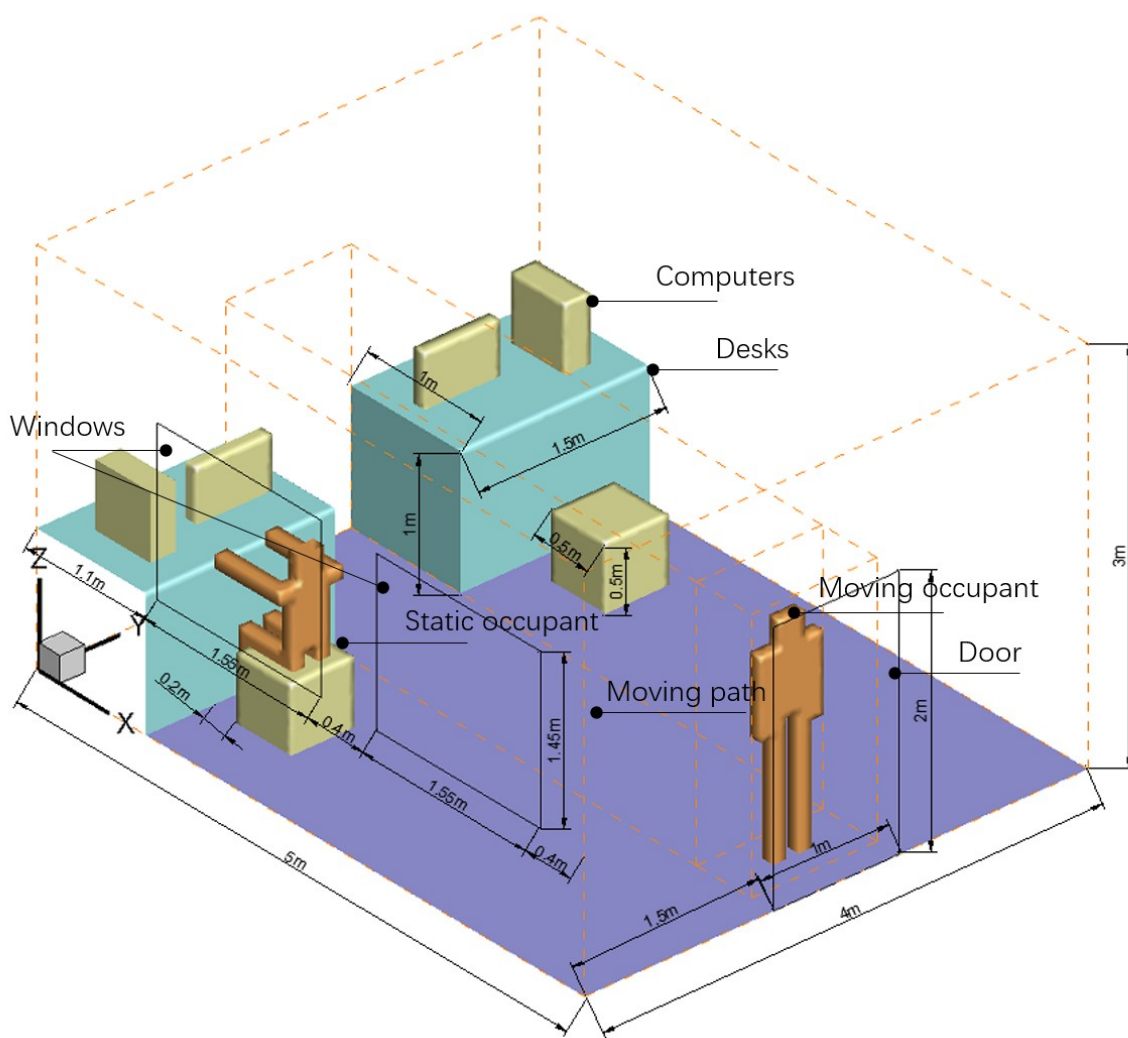


Figure 3. The geometrical features of the office room. There are two desks (1.0 m × 0.5m × 0.7 m in length × width × height) at one side of the room (5 m × 4 m × 3 m in length × width × height). One occupant remains sitting in front of the desk, the other one (1.75 m-height) walks through the door (2 m × 1 m in height × width), which is on the other side of the room. There are two windows (1.55 m × 1.45 m in width × height) on the side wall, which is adjacent to the seated occupant. The diffuser outlet of the HVAC (0.3 m × 0.2 m in width × height) is at the top of the wall towards the door. The lighting fixture is at the center of the ceiling.

UDF setting. The UDF (user-defined function) setting is a very important link in the overall framework, serving as a “bridge” connecting the outdoor and indoor concentration conditions, as well as taking the occupant behavior into consideration. The aforementioned generated occupant-related schedules determined both the natural and mechanical ventilation strategies (such as opening and closing time, as well as the air flow rate and its temperature etc.), these strategies were implemented in the CFD simulation as “time-series data” through coding the user-defined function. The natural ventilation strategy in Newsham’s research (Newsham 1994) is adopted in this work (open at arrival or when the outdoor environment is suitable, close at arrival, departure or when the outdoor environment is not suitable). Thus, when the windows were opened, the gaseous and particulate pollutants were blown into the room through the windows and the doors, where the velocity and temperature of the inlet airflow were set as the EnergyPlus modeling results. As for the mechanical ventilation strategy, it is a combination of availability schedule and actual window operation (when the window is open, the HVAC system will be off; when the window is closed, the HVAC system will be on if occupants feel hot). While the HVAC system was on, the windows

and the door, as well as the outdoor air system of the HVAC system, were all considered to be closed. The air purification system was assumed to be active in this work, with a removal rate of 50%. Thus, the gaseous composition and the corresponding concentrations of the next timestep's inlet airflow were calculated and input in the UDF code, according to the 50% concentration of reduced pollutants of the last timestep around the HVAC outlet. The air temperature and velocity of the inlet airflow were also set using the EnergyPlus modeling results. As for the movement behavior, the walking speed of the occupant was set to 1 m/s, and it took 5 s walking from the door to his seat (same in the opposite direction).

Calculation of IAQ index. The IAQ index is an index developed by the United States Environmental Protection Agency (EPA) that is used to indicate the indoor air quality in terms of its adverse health effects. On one side, the pollutant concentrations can be converted into the index value based on an empirical piecewise linear function. The breakpoints of specific pollutants are guided in the reports released by WHO in 2005 and 2010 (World Health Organization 2005; 2010). On the other side, the calculated index values are corresponding to different levels of adverse health symptoms based on many previous epidemiological studies and surveys. The IAQ index for each pollutant can be calculated from the modeled pollutant concentration results, as shown in Eq. 1.

$$I_p = \frac{I_{Hi} - I_{Lo}}{BP_{Hi} - BP_{Lo}} (C_p - BP_{Lo}) + I_{Lo} \quad (1)$$

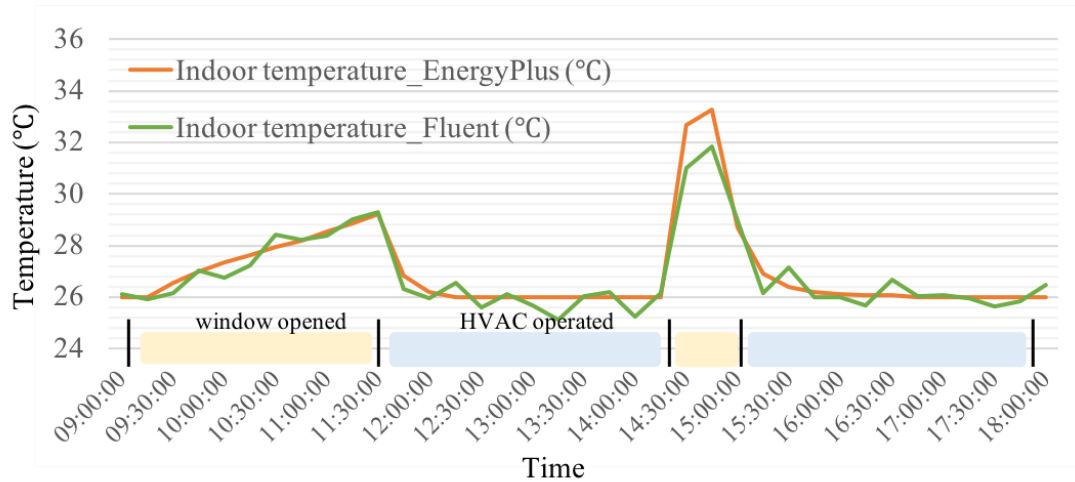
289where I_P is the index for pollutant P , C_P is the rounded concentration of
290pollutant P , BP_{Hi} is the breakpoint that is greater than or equal to C_P , BP_{Lo} is
291the breakpoint that is less than or equal to C_P , I_{Hi} is the AQI value
292corresponding to BP_{Hi} , and I_{Lo} is the AQI value corresponding to BP_{Lo} .
293According to the aforementioned concentration distribution, the average
294potential inhaled concentration was calculated within the vertical plane in
295front of the static human. The corresponding air quality level was then
296calculated based on Eq. 1. While the final AQI is the highest value calculated
297for each pollutant (Shi et al. 2015).

298

299**Results**

300**Verification of the consistency of the two simulations.** It was assumed
301that the occupant-related schedules remained the same in the two simulated
302environments of EnergyPlus and Fluent, making the process consistent. Due
303to the model that we employed in the obFMU, decision making regarding the
304operations of windows and HVAC was largely dependent on the indoor
305environment, especially room air temperature. Thus, to verify the
306consistency of the two simulated environments, indoor average temperature
307was chosen as the parameter for comparison. Figure 4 shows the indoor
308temperature modeled in EnergyPlus and Fluent, respectively. The occupant-

309related schedules generated in EnergyPlus were proved to be reasonable for
 310the indoor environment simulated in Fluent.



311

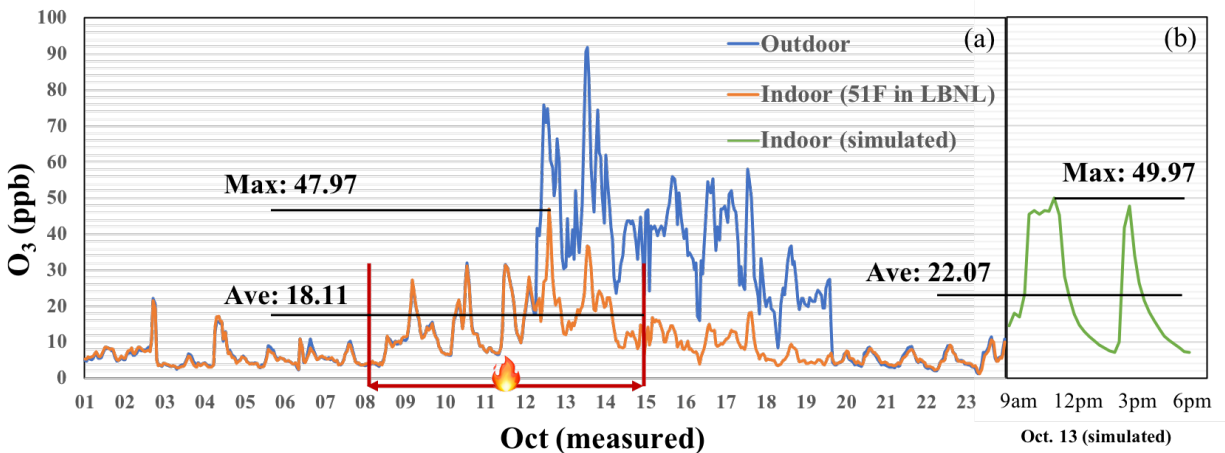
312**Figure 4. The indoor temperature simulated in EnergyPlus and**
 313**Fluent.** For EnergyPlus and Fluent simulations, indoor temperature both
 314rose slowly till around 29.2 °C before 11:30 am, when the windows were
 315opened. Then, the temperature remained at around 26.0 °C until 2:30 pm
 316within the duration when the HVAC was turned on. The same phenomenon
 317appeared for such behaviours afterward. Thus, the occupant-related
 318schedules generated in EnergyPlus were reasonable for the indoor
 319environment simulated in Fluent.

320

321**IAQ from measured data and simulated results.** The indoor and outdoor
 322air qualities before and after this wildfire event were provided by the Indoor
 323Environment Group at Lawrence Berkeley National Laboratory (LBNL). Some
 324office rooms inside the Building 51F in Lawrence Berkeley National
 325Laboratory (LBNL) are serving as a living laboratory to continually monitor
 326the indoor and outdoor carbon dioxide and pollutant concentrations (e.g.,
 327ozone, particular matters). Figures 5-6 show the comparisons of IAQ level
 328(namely ozone and PM2.5) between the measured and simulated results.
 329Since more detailed IAQ measurement was not available, we chose the

average and maximum concentration levels as the comparison indexes of the measured and simulated results. From Oct. 8 to Oct. 15, 2017, IAQ worsened after the breakout of the wildfire, and continued for the next whole week (Figure 5 (a)). During this week, the average concentration level of the indoor ozone was 18.11 ppb. The maximum levels of the ozone reached 47.97 ppb on October 12, 2017, when the outdoor quality data was 76 ppb. The simulated average and maximum levels of ozone in Figure 5 (b) were overall consistent with the measured results, except for two details. First, ozone is a highly reactive component that reacts quickly with surfaces when penetrating indoors, which is why the measured ozone levels are generally lower than those modeled levels. Second, the measured indoor ozone level stayed at 10 ppb during the night when all unintentional openings of the building were closed, during which time, the simulated result was almost zero. These differences between the measured and modeled results were supposed to be associated with air infiltration in the building and are further discussed in the discussion section.

346



347

348 **Figure 5 Comparison of the measured and simulated O₃ levels.** (a)
 349 Concentration of Ozone measured indoors and outdoors, before, during and after
 350 the wildfire. (b) The simulated concentration of the indoor Ozone on Oct. 13.
 351

352 Measured data of particle levels from October 12 to 14 indicate that the
 353 maximum and average levels of PM_{2.5} were 91.97 ug/m³ and 51.44 ug/m³,
 354 respectively (Figure 6 (a)), while those of the simulated results were 131.49
 355 ug/m³ and 53.02 ug/m³, respectively (Figure 6 (b)). The simulated results
 356 were a little higher than the measured data, which might be due to less
 357 consideration of the particle interaction. Comparing to the outdoor
 358 concentration, the indoor PM was about 65% of the outdoor level on average,
 359 under an air exchange rate of 0.7 air changes per hour in this work.

360

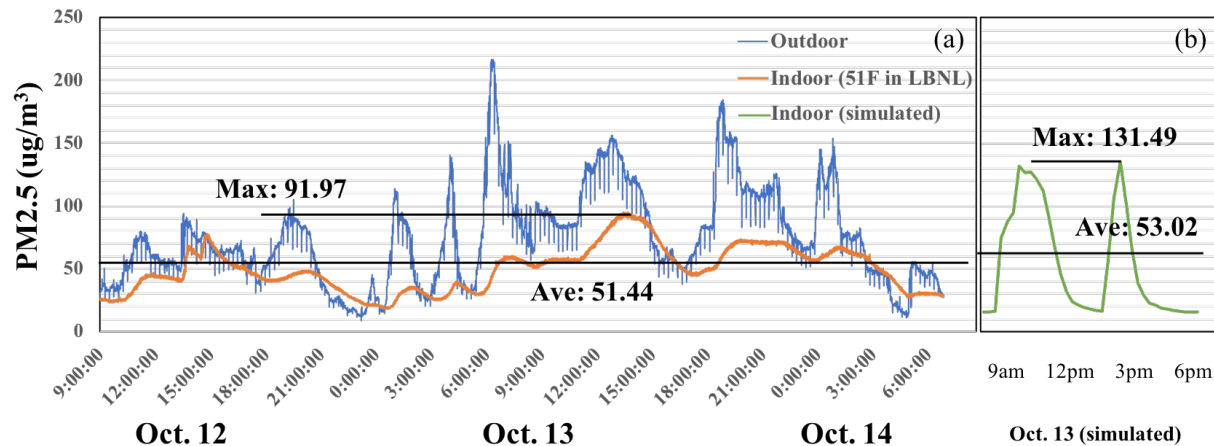


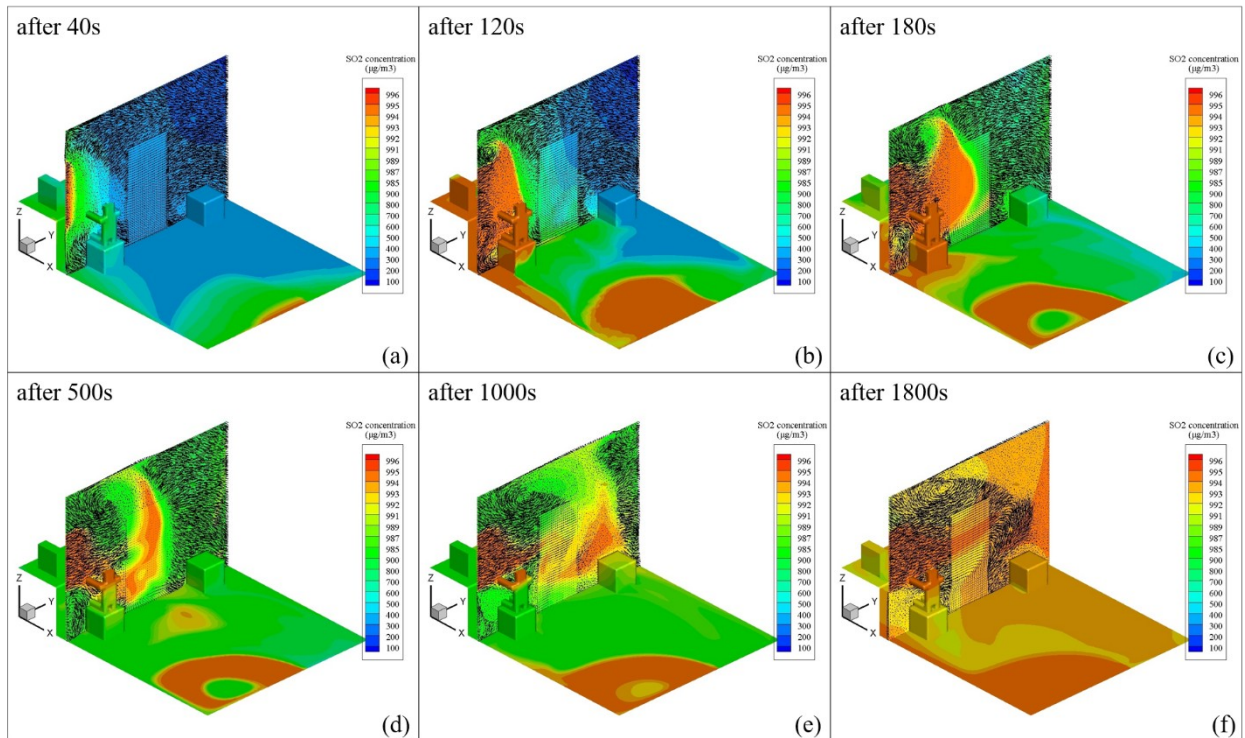
Figure 6 Comparison of the measured and simulated PM2.5 levels.
 (a) Concentration of PM2.5 measured indoors and outdoors during the wildfire. (b) The simulated concentration of the indoor PM2.5 on Oct. 13.

The fluctuant simulated results indicated that occupant behaviors exerted a large influence on the indoor pollutant concentration during the working hours. Through the comparison, the fluctuant indoor concentration level was proved to be consistent with the measured data in the actual office environment if the occupant behaviors were considered during the simulation.

Flow pattern and concentration distribution. The plane in front of the oronasal ($x=1.25\text{m}$, see Figure 3) region was chosen as the potential inhalation region. The evolution of the flow structure and the concentrations of different gaseous pollutants in this region may largely influence human inhalation doses, which is significant in assessing exposure risk levels. According to the aforementioned outdoor air quality on that day, the outdoor concentration of sulfur dioxide (SO_2) was much higher than an average day,

380 and its hazard level was higher than that of carbon monoxide and ozone.
 381 Thus, sulfur dioxide was chosen as the representative pollutant to
 382 investigate its diffusion characteristics.

383



384

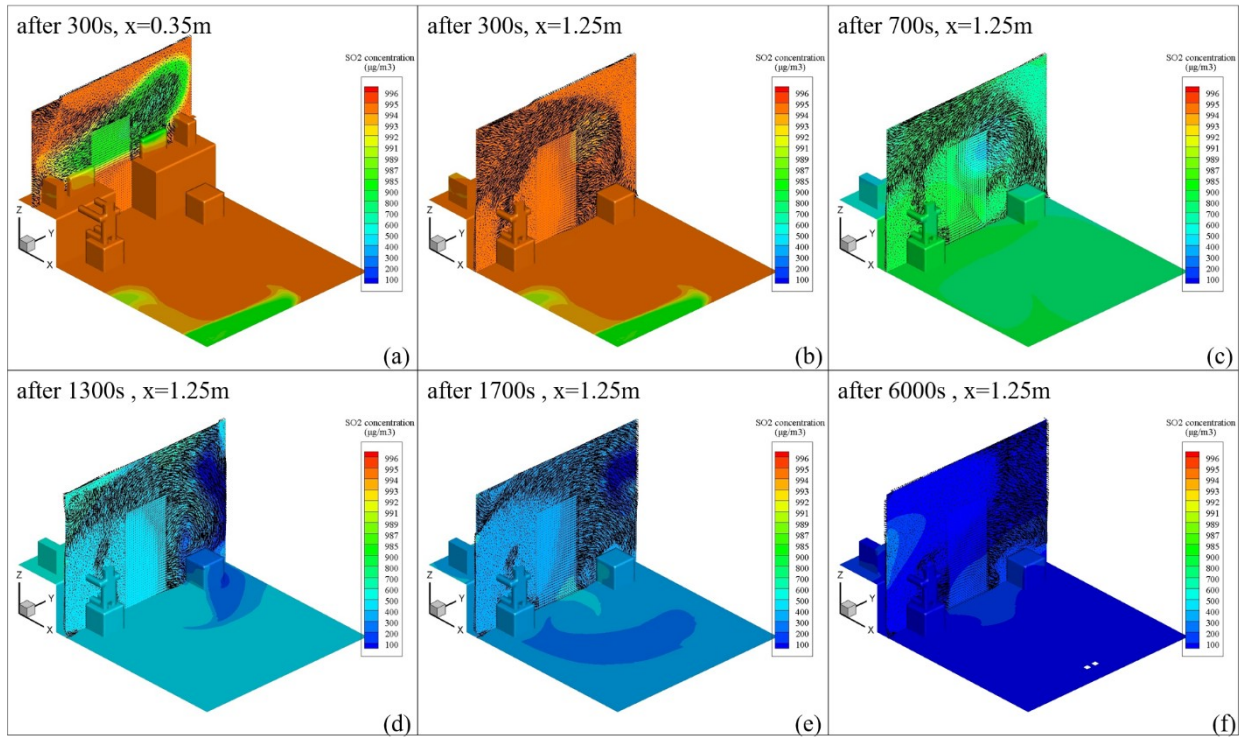
385 **Figure 7 The velocity and concentration fields of SO₂ indoors after**
 386 **the windows were opened. (a) At inhalation plane, 40s after the window was**
 387 **opened. (b) After 120s. (c) After 180s. (d) After 500s. (e) After 1000s. (f) After**
 388 **1800s.**

389

390 Operation of windows exerted a significant impact on flow pattern and
 391 concentration distribution (Figure 7). Outdoor sulfur dioxide was diffused
 392 quickly through the windows. Owing to the short distance between the
 393 seated occupant and the windows, the concentration of the sulfur dioxide
 394 near the oro-nasal region reached a relatively high level just after 120s
 395 (Figure 7 (b)). The inlet airflow was affected by transient outdoor weather

396data, such as wind velocity and direction outdoors. Meanwhile, the diffusion
397of the inlet airflow was also influenced by the existent indoor airflow
398circulation. Eventually, the concentration of sulfur dioxide remained at a
399steady state after 30 min, which was around 995 ug/m^3 (348.25 ppb). Due to
400the same pattern of the velocity field, concentration evolutions for carbon
401monoxide and ozone were similar to that of the sulfur dioxide. Eventually,
402after 30 min of opening the windows, concentrations of indoor carbon
403monoxide and ozone on the inhalation region ($x=1.25 \text{ m}$) reached around
404 1.40 mg/m^3 (1.12 ppm) and 107.08 ug/m^3 (49.97 ppb), respectively.

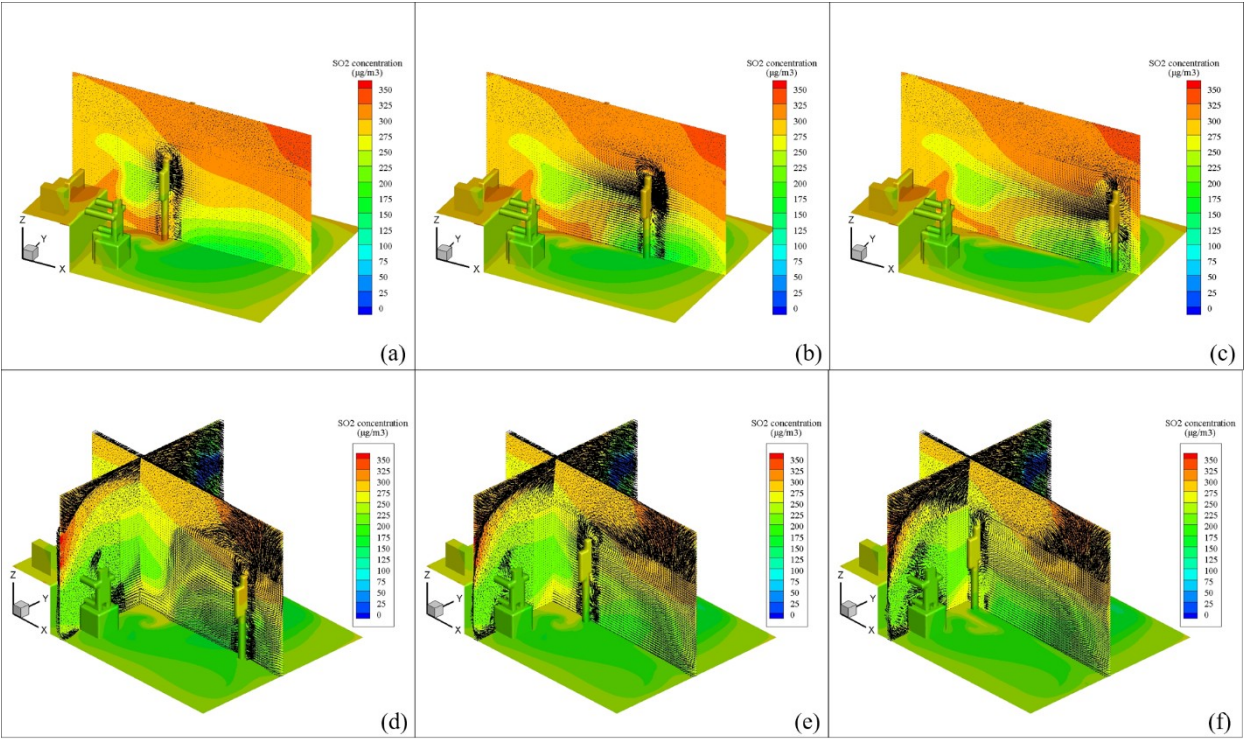
405 Flow pattern and concentration distribution caused by other occupant
406behaviors such as air-conditioning and movement can be found in Figure 8-9.
407The velocity and concentration fields on the plane near the HVAC outlet 300
408s after the HVAC was turned on, indicated the effects of the HVAC operation
409on the IAQ (Figure 8 (a)). The cold air coming from the HVAC outlet moved
410downwards during the diffusion (Figure 8 (b-f)). 1300 s after the HVAC
411operation, the concentration of indoor sulfur dioxide dropped to 500 ug/m^3 .
412And 6000 s after the HVAC operation, the concentration of sulfur dioxide
413remained at a relatively steady state, which was around 100 ug/m^3 .
414Combined with the aforementioned analysis, occupants are advised to keep
415the windows closed and run the HVAC systems with the outdoor air dampers
416shutting off during wildfire to mitigate the indoor exposure risk.



417
 418 **Figure 8 The velocity and concentration fields of SO₂ indoors after**
 419 **the HVAC was turned on. (a) At the plane near the HVAC outlet, 300 s**
 420 **after the HVAC was operated. (b) At inhalation plane, 300 s after the HVAC**
 421 **was operated. (c) After 700 s. (d) After 1300 s. (e) After 1700 s. (f) After**
 422 **6000 s.**
 423

424 The effects of the occupant movements, i.e. walking out of and into the
 425 room, can be found in Figure 9 (a-c) and (d-f), respectively. A strong
 426 downward airflow was observed behind its upper body, carrying the gaseous
 427 pollutant downwards; while the gap between the lower limbs exerted a
 428 horizontal flow between the legs, which enhanced the diffusion speed of the
 429 pollutants. The detailed information of the velocity fields evaluated in this
 430 study has been verified in a previous PIV experimental study (Luo et al.
 431 2018a). Overall, the movement behavior accelerated the diffusion and
 432 mixture of the existed contaminants at different heights, which enhanced the

433risk of respiratory exposure. Therefore, occupants are recommended to limit
 434walking activities during the extreme wildfires.



435
 436**Figure 10 The velocity and concentration fields of SO₂ along the**
 437**moving. (a-c) The occupant was walking out of the office. (d-f) The**
 438**occupant was walking into the room.**
 439

440**Assessment of the daily exposure risk level.** Epidemiological studies
 441have linked exposure to indoor air pollution with a wide range of adverse
 442health outcomes. The health effects and the breakpoints of some specific
 443pollutants considered in this study are listed in Table 2 (documented from
 444(WHO 2010; Mintz 2013; World Health Organization 2005)).

445**Table 2. Pollutant-specific sub-indices and health effects statements**
 446**for guidance on the AQI.** The IAQ index for each pollutant can be
 447calculated from the modeled pollutant concentration results, seen in
 448Methods.

AQI Categorie s: Index	Ozone (ppb)		Sulfur Dioxide (ppb)		Carbon Monoxide (ppm)	Particulate Matter (ug/m ³) [24-hour]
	[1-hour]	[8-hour]	[1-hour]	[24-		

Values				hour]		
Good (Up to 50)	-	0-59 None	0-35	0-30	[8-hour] 0-4.4	0-12.0 None
			None			
Moderate (51-100)	-	60-75 Unusually sensitive individuals may experience respiratory symptoms	36-75	>30- 140	4.4-9.4 None	12.1-35.4 Respiratory symptoms possible in unusually sensitive individuals; possible aggravation of heart or lung disease in people with cardiopulmonary disease and older adults
	125-164	76-95	76-185	140- 220	9.5-12.4 Increasing likelihood of reduced exercise tolerance due to increased cardiovascular symptoms, such as chest pain, in people with heart disease	35.5-55.4 Increasing likelihood or respiratory symptoms in sensitive individuals; aggravation of heart or lung disease and premature mortality in people with cardiopulmonary disease, older adults, and people of lower SES
Unhealthy for Sensitive Groups (101-150)	Increasing likelihood of respiratory symptoms and breathing discomfort in people with lung disease, such as asthma, children, older adults, and outdoor workers		Increasing likelihood of respiratory symptoms, such as chest tightness and breathing discomfort in people with asthma			
	165-204	96-115	186- 304	220- 300	12.5-15.4 Reduced exercise tolerance due to increased cardiovascular symptoms, such as chest pain, in people with heart disease	55.5-150.4 Increased aggravation of heart or lung disease and premature mortality in people with cardiopulmonary disease, older adults, and people of lower SES; increased respiratory effects in general population
Unhealthy (151-200)	Greater likelihood of respiratory symptoms and breathing difficulty in people with lung disease, such as asthma, children, older adults, and outdoor workers; possible respiratory effects in general population		Increased respiratory symptoms, such as chest tightness and wheezing in people with asthma; possible aggravation of other lung disease			
	205-404	116-374	305- 604	300- 600	15.5-30.4 Significant aggravation of cardiovascular symptoms, such as chest pain, in people with heart disease	150.5-250.4 Significant aggravation of heart or lung disease and premature mortality in people with cardiopulmonary disease, older adults, and people of lower SES; significant increased respiratory effects in general population
Very Unhealthy (201-300)	Increasing severe symptoms and impaired breathing likely in people with lung disease, such as asthma, children, older adults, and outdoor workers; increasing likelihood of respiratory effects in general population		Significant increase in respiratory symptoms, such as wheezing and shortness of breath, in people with asthma; aggravation of other lung diseases			
Hazardou s (301-500)	405-604	-	605- 1004	600- 1000	30.5-50.4 Serious aggravation of cardiovascular symptoms, such as chest pain, in people with heart disease; impairment of strenuous activities in general population	250.5-500.4 Serious aggravation of heart or lung disease and premature mortality in people with cardiopulmonary disease, older adults, and people of lower SES; serious risk of respiratory effects in general population

450 According to the modeled concentration results, where the 1-hour SO₂
451value was 348.25 ppb, CO value was 1.12 ppm, the O₃ value was 47.97 ppb,
452and the PM_{2.5} value was 131.49 ug/m³, the calculated maximum IAQ index
453was 215, with SO₂ as the responsible pollutant. Qualitative evaluation
454indicated that this environment would cause an increasing likelihood of
455respiratory symptoms, such as wheezing, chest tightness and breathing
456discomfort in people with asthma, as well as an increasing aggravation of
457other lung diseases. However, to achieve the quantitative evaluation of the
458injury level, further analyses should be conducted considering an entering
459path of the particle and gaseous contaminants into the body through
460breathing. The modeled dynamic indoor contaminant concentration can be
461served as a boundary condition.

462 As for the impact of occupant behaviors on the daily exposure risk level,
463due to the distribution of different indoor occupant behaviors, the indoor
464pollutant concentration fluctuated obviously during the working hours.
465Activities such as opening the windows as well as walking into and out of the
466rooms led to the increase of the pollutant concentration and thus the
467exposure risk of the human body and respiratory. While turning on the air-
468conditioning without the function of supplying fresh air decreased the indoor
469contaminant concentration in a slow but effective way. Therefore, to mitigate
470indoor exposure risk, occupants are advised to keep windows closed and
471limit walking activities during the extreme wildfires. Meanwhile, outdoor air
472dampers should be shutting off when operating the HVAC system to avoid

473more purification loads. From another aspect, a proper and accurate set of
474occupant behavior schedules and the corresponding building boundary
475conditions are also crucial for enhancing the evaluation and prediction of the
476indoor risk exposure.

477**Discussions**

478This study formulated a framework for the indoor pollutants exposure
479modeling and the potential human health hazard assessment in an office
480environment particularly taking into account the actual occupant behaviours.
481The simulated results under this framework were compared with the actual
482measured indoor and outdoor data (O_3 and $PM_{2.5}$), showing great
483consistency in both the maximum and average levels. The indoor airflow
484pattern and IAQ fluctuated obviously within working hours, which were
485largely dependent on specific occupant behaviors. Therefore, comparing to
486the traditional IAQ and occupant exposure assessments when occupants
487remained static or the indoor equipment (e.g., HVAC and windows) remained
488constant running, the framework in this study is proved to provide a more
489realistic and reliable result aligned with the actual requirement of assessing
490the health hazard level of the indoor occupants. Furthermore, based on this
491result as a boundary condition, the deposit fraction and equation can be
492fitted to predict a more accurate and dynamic respiratory exposure dosage
493under such outdoor wildfire conditions, which not only indicates the key
494injury level, but also provides reference for the further physiological stage.

495**Assessment of the respiratory injury**

As aforementioned, the indoor pollutant concentration near the oro-nasal could be considered as the boundary condition for assessing the respiratory deposition. Take nasal inhalation as an example, respiratory injury was mainly caused by the micron particle deposition fraction in nasal cavity, pharynx, larynx and trachea regions for nasal breathing. The detailed modelling method and flow pattern inside the respiratory system were included in another published journal article (Xu et al. 2018).

The simulated particle size range was slightly expanded to allow a wider coverage of the developed deposition equations. For micron-sized particles, deposition fractions were related to the inertial parameter I , which considered particles mass to the square power, and the averaged fluid momentum. The inertial parameter is defined as:

$$I = d_p^2 Q \quad (2)$$

where Q is the volume flow rate (cm^3/s) and d_p (μm) is the particle aerodynamic diameter. Figure 11(a) and (c) show the deposition fraction in human respiratory airways for particles ranging from $0.8 \mu\text{m}$ to $20 \mu\text{m}$ against the inertial parameter for oral and nasal inhalation, respectively.

The Stokes number was used to correlate the deposition to length scale, particle density, size and flow rate. It is defined as:

$$St = \frac{\rho_p d_p^2 u C_c}{18 \mu L} \quad (3)$$

516 where L is the characteristic length of oral and u is the local airflow
 517 velocity. The deposition through oral breathing in human airway was related
 518 to St and Re .

519 For the deposition equation in human airway, improved fittings were
 520 obtained with $St^{3.271}Re$ and $St^{1.77}Re^{0.145}$ for particle sizes from 0.8 to 20 μm ,
 521 breathing rate of 10 and 30 L/min for oral and nasal breathing (Figure 11(b)
 522 and (d)), with a coefficient of determination $R^2=0.99$. The empirical
 523 equations are given as

$$524 \quad DF_{oral} = [1 - \frac{0.956}{22.701 St^{3.271} Re + 1}] \times 100\% \quad (4)$$

$$525 \quad DF_{nasal} = [1 - 0.95 \exp(-7.35 \cdot St^{1.77} Re^{0.145})] \times 100\% \quad (4)$$

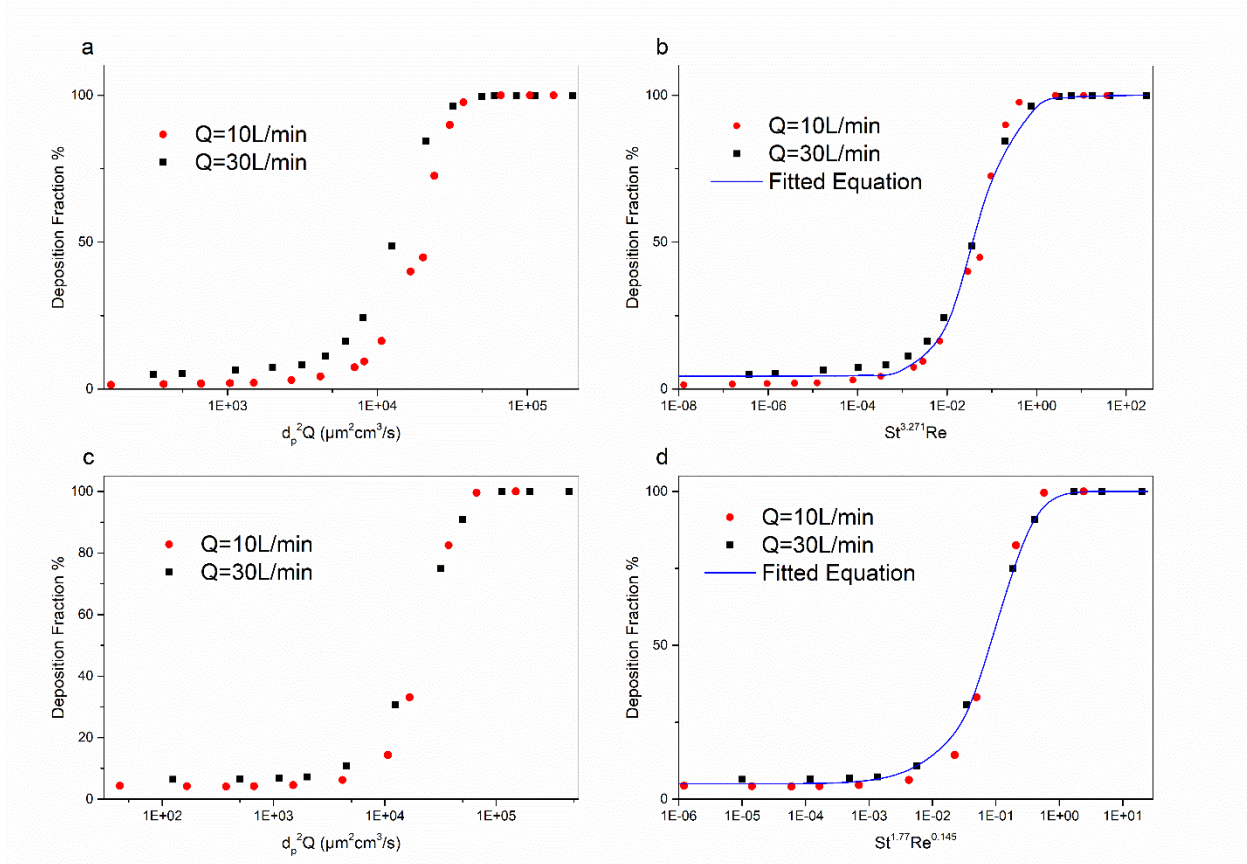


Figure 11 Comparison of micron particles (0.8 – 20 μm). (a) deposition fraction for oral inhalation. (b) fitted deposition equation for oral inhalation. (c) deposition fraction for nasal inhalation. (d) fitted deposition equation for nasal inhalation.

531

The dosimetry (in number, mass, surface area) in human upper airway under various breathing flow rates and breathing pattern was calculated by using the above simulated PM_{2.5} concentration value, presented in Table 3. The time period of occupants staying indoors was assumed as 8 hours a day (as the working hours from 9am to 5pm). A monotonous growth was obtained in human upper airway dosimetry with the flow rate, which lead to a larger air exchange and particle exposure risk, as well as a higher probability of chronic respiratory diseases.

Table 3 Human upper airway dosages of indoor PM_{2.5} during a day.

Q (L/min)	Oral inhalation			Nasal inhalation		
	Number (10 ⁶ #)	Mass(μ g)	Surface area (10 ⁻⁵ m ²)	Number (10 ⁶ #)	Mass(μ g)	Surface area (10 ⁻⁵ m ²)
10	2.93	23.96	5.75	6.41	52.16	12.60
30	36.25	296.6	71.18	31.11	255.3	61.15

541

542 Limitations

One limitation of this work is that air infiltration via building permeability (e.g., windows, envelope cracks) was not considered during the CFD simulation. Several previous studies (Shi et al. 2015; G. Hong and Kim 2016; C. Chen and Zhao 2011) have proved the effects of air infiltration on IAQ and verified the infiltration factor as the useful parameter for qualifying the number of indoor particles infiltrating from the outdoor environment. To

549 evaluate the potential effect of building permeability on the current results,
550 we estimate the average infiltration rate as 0.2 air changes per hour (ACH) in
551 summer based on some previous research (Chen and Zhao 2011; G. Hong
552 and Kim 2016). According to the volume of the room and the outdoor
553 pollutant concentration, the air infiltration process might cause the indoor
554 ozone level to raise to 8 ppb during the night. As can be seen in Figure 5, the
555 measured indoor ozone concentration stayed around 10 ppm during the
556 night when the windows were closed, which was supposed to be associated
557 with the air infiltration. Therefore, the actual indoor pollutant concentration
558 considering the air infiltration would be 5% higher than the simulated results
559 in this work, which results in a higher IAQ index and thus higher exposure
560 risk than evaluated.

561 As for the concept of the exposure injury, in the current work, we focus
562 more on the indoor air quality and the corresponding respiratory dosage and
563 deposition through breathing. As concluded in Table 2, a qualitative
564 evaluation indicates the significant potential of wheezing and shortness of
565 breath in people with asthma, as well as the increasing of lung disease,
566 under the calculated IAQ index. However, quantitative analysis of the
567 contaminant penetrating into the blood through layers of skin, stratum
568 corneum, viable epidermis and dermal capillaries is also necessary to carry
569 out together with the physiological researches in the next step, to determine
570 the exact injury level. Recently, a model of transdermal uptake of hazardous
571 chemicals has been raised by Morrison et al. in 2017. The final mass of the

gaseous chemicals (e.g., SO₂, CO) entered the blood can be calculated based on the dynamic indoor chemical concentration as a boundary condition. But the key point is to validate the aforementioned model with a set of proper parameters for specific gaseous contaminants.

As for the selection of airborne particle metrics, ultrafine particles also play a non-negligible role in affecting the occupant health, especially to the respiratory system due to its smaller particle size (Ibald-Mulli et al. 2002; Zhao et al. 2009; Nikolova et al. 2011). Plus that the physical diffusion process (origin, dynamic and penetration) between PM_{2.5} and ultrafine particles are actually different. Therefore, the approach proposed in this work is a simplified approach for not considering the ultrafine particles in the overall framework. To address this problem, accurate measured ultrafine particles data should be collected via carefully designed experiments, to further validate the physical models of their diffusion process.

The methodology in this paper is more targeting at the commercial building types (namely, office buildings) where many indoor pollutant sources such as cooking and incense could be negligible. When it comes to residential building types for a broader application, the simulation of indoor combustion sources should be added to the current methodology, especially the CFD simulation of the origin, dynamics and penetration of such particle metrics (Yang and Ye 2014; Ezzati and Kammen 2001).

Conclusion

595 This work employed both whole-building simulation (EnergyPlus coupled with
596 obFMU) and computational fluid dynamics (Fluent) to analyze the impacts of
597 occupant behaviors (namely window operation, HVAC operation, and human
598 movements) on indoor airflow patterns and IAQ. The IAQ, especially
599 considering daily occupant behavior schedules, was assessed during the
600 period of a wildfire event in the Northern California, U.S.

601 The simulated results were compared with the actual measured indoor and
602 outdoor data (O₃ and PM_{2.5}). The measured and simulated IAQ were
603 consistent based on the maximum and average levels. The occupant
604 behaviors were proved to exert significant impacts on the indoor air flow
605 pattern and thus the pollutants' concentrations. The indoor airflow pattern
606 and IAQ transformed obviously within working hours, which were largely
607 dependent on occupant behaviors. Thus, to mitigate indoor exposure risk,
608 occupants are advised to keep windows closed and operate HVAC systems
609 without outdoor air. Besides, occupants' movements accelerate the diffusion
610 and mixture of existing contaminants at different heights, which could
611 enhance the risk of respiratory exposure. The daily maximum IAQ index was
612 215, with SO₂ as the responsible pollutant, which might result in significant
613 respiratory symptoms and adverse health effects, such as wheezing and
614 shortness of breath, in children, older adults, and people with asthma. Based
615 on indoor air conditions and considering occupant behaviors, deposit fraction
616 and equation were fitted to predict the respiratory injury level under such
617 outdoor wildfire conditions.

618This study formulated a framework for the indoor pollutants exposure
619modeling and the potential human health hazard assessment in an office
620environment while taking into account actual occupant behaviors. This co-
621simulation was conducted by combining the building energy modeling,
622occupant behavior modeling, CFD modeling, and pollutant modeling, which
623can be further applied in each IAQ issue where the outdoor-to-indoor
624pollutant penetration aspect is important (such as wildfire events as
625demonstrated in this work, haze pollution in China, as well as the vehicle
626exhaust etc). Results can be used to evaluate and inform strategies to
627mitigate occupant health conditions during outdoor events of extreme
628pollution.

629

630**References:**

- 631Anderson CM, Kissel KA, Field CB, Mach KJ (2018). Climate Change Mitigation,
632 Air Pollution, and Environmental Justice in California. *Environmental*
633 *Science & Technology*, 52(18): 10829–38.
- 634Chen C, Zhao B (2011). Review of Relationship between Indoor and Outdoor
635 Particles: I/O Ratio, Infiltration Factor and Penetration Factor.
636 *Atmospheric Environment*,.
637 <https://doi.org/10.1016/j.atmosenv.2010.09.048>.
- 638Chen Y, Hong T, Luo X (2018). An Agent-Based Stochastic Occupancy
639 Simulator. *Building Simulation*,. [https://doi.org/10.1007/s12273-017-](https://doi.org/10.1007/s12273-017-0379-7)
640 0379-7.

641Crawley DB, Lawrie LK, Winkelmann FC, Buhl WF, Huang YJ, Pedersen CO,
642 Strand RK, Liesen RJ, Fisher DE, Witte MJ, Glazer J (2001). EnergyPlus:
643 Creating a New-Generation Building Energy Simulation Program. *Energy*
644 *and Buildings*,. [https://doi.org/10.1016/S0378-7788\(00\)00114-6](https://doi.org/10.1016/S0378-7788(00)00114-6).

645Ezzati M, Kammen DM (2001). Quantifying the Effects of Exposure to Indoor
646 Air Pollution from Biomass Combustion on Acute Respiratory Infections in
647 Developing Countries. *Environmental Health Perspectives*, 109(5): 481–
648 88.

649Fracastoro GV, Mutani G, Perino M (2002). Experimental and Theoretical
650 Analysis of Natural Ventilation by Windows Opening. In *Energy and*
651 *Buildings*,. [https://doi.org/10.1016/S0378-7788\(02\)00099-3](https://doi.org/10.1016/S0378-7788(02)00099-3).

652Gosselin JR, Chen Q (Yan) (2008). A Computational Method for Calculating
653 Heat Transfer and Airflow through a Dual-Airflow Window. *Energy and*
654 *Buildings*,. <https://doi.org/10.1016/j.enbuild.2007.03.010>.

655Haddrell AE, Davies JF, Reid JP (2015). Dynamics of Particle Size on Inhalation
656 of Environmental Aerosol and Impact on Deposition Fraction.
657 *Environmental Science and Technology*,.
658 <https://doi.org/10.1021/acs.est.5b01930>.

659Haikerwal A, Akram M, Monaco A Del, Smith K, Sim MR, Meyer M, Tonkin AM,
660 Abramson MJ, Dennekamp M (2015). Impact of Fine Particulate Matter
661 (PM_{2.5}) Exposure during Wildfires on Cardiovascular Health Outcomes.
662 *Journal of the American Heart Association*,.
663 <https://doi.org/10.1161/JAHA.114.001653>.

664Haldi F (2013). A Probabilistic Model To Predict Building Occupants' Diversity
 665 Towards Their Interactions With the Building Envelope. *Proceedings of*
 666 *the International IBPSA Conference*,.

667Han Z, Weng W, Huang Q (2014). Numerical and Experimental Investigation
 668 on the Dynamic Airflow of Human Movement in a Full-Scale Cabin. In
 669 *HVAC and R Research*,. <https://doi.org/10.1080/10789669.2014.882677>.

670Hong G, Kim BS (2016). Field Measurements of Infiltration Rate in High Rise
 671 Residential Buildings Using the Constant Concentration Method. *Building*
 672 *and Environment*,. <https://doi.org/10.1016/j.buildenv.2015.11.027>.

673Hong T, D'Oca S, Taylor-Lange SC, Turner WJN, Chen Y, Corngati SP (2015).
 674 An Ontology to Represent Energy-Related Occupant Behavior in
 675 Buildings. Part II: Implementation of the DNAS Framework Using an XML
 676 Schema. *Building and Environment*,.
 677 <https://doi.org/10.1016/j.buildenv.2015.08.006>.

678Hong T, D'Oca S, Turner WJN, Taylor-Lange SC (2015). An Ontology to
 679 Represent Energy-Related Occupant Behavior in Buildings. Part I:
 680 Introduction to the DNAs Framework. *Building and Environment*,.
 681 <https://doi.org/10.1016/j.buildenv.2015.02.019>.

682Hong T, Sun H, Chen Y, Taylor-Lange SC, Yan D (2016). An Occupant
 683 Behavior Modeling Tool for Co-Simulation. *Energy and Buildings*,.
 684 <https://doi.org/10.1016/j.enbuild.2015.10.033>.

685Hong T, Yan D, D'Oca S, Chen C fei (2017). Ten Questions Concerning
 686 Occupant Behavior in Buildings: The Big Picture. *Building and*

687 *Environment*,. <https://doi.org/10.1016/j.buildenv.2016.12.006>.

688 Hurteau MD, Westerling AL, Wiedinmyer C, Bryant BP (2014). Projected
 689 Effects of Climate and Development on California Wildfire Emissions
 690 through 2100. *Environmental Science & Technology*, 48(4): 2298–2304.

691 Ibald-Mulli A, Wichmann H-E, Kreyling W, Peters A (2002). Epidemiological
 692 Evidence on Health Effects of Ultrafine Particles. *Journal of Aerosol
 693 Medicine*, 15(2): 189–201.

694 Jaffe DA, Wigder N, Downey N, Pfister G, Boynard A, Reid SB (2013). Impact
 695 of Wildfires on Ozone Exceptional Events in the Western US.
 696 *Environmental Science & Technology*, 47(19): 11065–72.

697 Jolly WM, Cochrane MA, Freeborn PH, Holden ZA, Brown TJ, Williamson GJ,
 698 Bowman DMJS (2015). Climate-Induced Variations in Global Wildfire
 699 Danger from 1979 to 2013. *Nature Communications*, 6: 7537.

700 Klepeis NE, Nelson WC, Ott WR, Robinson JP, Tsang AM, Switzer P, Behar J V,
 701 Hern SC, Engelmann WH (2001). The National Human Activity Pattern
 702 Survey (NHAPS): A Resource for Assessing Exposure to Environmental
 703 Pollutants. *Journal of Exposure Science and Environmental Epidemiology*,
 704 11(3): 231.

705 Lewis TC, Robins TG, Mentz GB, Zhang X, Mukherjee B, Lin X, Keeler GJ,
 706 Dvonch JT, Yip FY, O'Neill MS (2013). Air Pollution and Respiratory
 707 Symptoms among Children with Asthma: Vulnerability by Corticosteroid
 708 Use and Residence Area. *Science of the Total Environment*, 448: 48–55.

709 Lin B, Huangfu Y, Lima N, Jobson B, Kirk M, O'Keeffe P, Pressley S, Walden V,

710 Lamb B, Cook D (2017). Analyzing the Relationship between Human
 711 Behavior and Indoor Air Quality. *Journal of Sensor and Actuator*
 712 *Networks*,. <https://doi.org/10.3390/jsan6030013>.
 713 Luo N, Weng W, Xu X, Fu M (2018a). Experimental and Numerical
 714 Investigation of the Wake Flow of a Human-Shaped Manikin: Experiments
 715 by PIV and Simulations by CFD. *Building Simulation*,.
 716 <https://doi.org/10.1007/s12273-018-0446-8>.
 717 ——— (2018b). Human-Walking-Induced Wake Flow – PIV Experiments and
 718 CFD Simulations. *Indoor and Built Environment*,.
 719 <https://doi.org/10.1177/1420326X17701279>.
 720 Luongo JC, Fennelly KP, Keen JA, Zhai ZJ, Jones BW, Miller SL (2016). Role of
 721 Mechanical Ventilation in the Airborne Transmission of Infectious Agents
 722 in Buildings. *Indoor Air*,. <https://doi.org/10.1111/ina.12267>.
 723 Mintz D (2013). Technical Assistance Document for the Reporting of Daily Air
 724 Quality – the Air Quality Index (AQI). *Environmental Protection*,.
 725 Montgomery JF, Storey S, Bartlett K (2015). Comparison of the Indoor Air
 726 Quality in an Office Operating with Natural or Mechanical Ventilation
 727 Using Short-Term Intensive Pollutant Monitoring. *Indoor and Built*
 728 *Environment*,. <https://doi.org/10.1177/1420326X14530999>.
 729 Morrison GC, Weschler CJ, Bekö G (2017). Dermal Uptake of Phthalates from
 730 Clothing: Comparison of Model to Human Participant Results. *Indoor Air*,.
 731 <https://doi.org/10.1111/ina.12354>.
 732 Navarro KM, Cisneros R, O'Neill SM, Schweizer D, Larkin NK, Balmes JR

733 (2016). Air-Quality Impacts and Intake Fraction of PM_{2.5} during the 2013
 734 Rim Megafire. *Environmental Science & Technology*, 50(21): 11965–73.
 735 Newsham GR (1994). Manual Control of Window Blinds and Electric Lighting:
 736 Implications for Comfort and Energy Consumption. *Indoor and Built*
 737 *Environment*,. <https://doi.org/10.1177/1420326X9400300307>.
 738 Nikolova I, Janssen S, Vos P, Vrancken K, Mishra V, Berghmans P (2011).
 739 Dispersion Modelling of Traffic Induced Ultrafine Particles in a Street
 740 Canyon in Antwerp, Belgium and Comparison with Observations. *Science*
 741 *of the Total Environment*, 412: 336–43.
 742 Shi S, Chen C, Zhao B (2015). Air Infiltration Rate Distributions of Residences
 743 in Beijing. *Building and Environment*,.
 744 <https://doi.org/10.1016/j.buildenv.2015.05.027>.
 745 Stabile L, Dell’Isola M, Russi A, Massimo A, Buonanno G (2017). The Effect of
 746 Natural Ventilation Strategy on Indoor Air Quality in Schools. *Science of*
 747 *the Total Environment*,. <https://doi.org/10.1016/j.scitotenv.2017.03.048>.
 748 West JJ, Smith SJ, Silva RA, Naik V, Zhang Y, Adelman Z, Fry MM, Anenberg S,
 749 Horowitz LW, Lamarque J-F (2013). Co-Benefits of Mitigating Global
 750 Greenhouse Gas Emissions for Future Air Quality and Human Health.
 751 *Nature Climate Change*, 3(10): 885.
 752 WHO (2010). WHO Guidelines for Indoor Air Quality: Selected Pollutants.
 753 Bonn, Germany: In Puncto Druck+ Medien GmbH,.
 754 <https://doi.org/10.1186/2041-1480-2-S2-I1>.
 755 World Health Organization (2005). WHO Air Quality Guidelines for Particulate

756 Matter, Ozone, Nitrogen Dioxide and Sulfur Dioxide: Global Update 2005.
 757 *World Health Organization*,. [https://doi.org/10.1016/0004-](https://doi.org/10.1016/0004-6981(88)90109-6)
 758 6981(88)90109-6.

759 Xu X, Shang Y, Tian L, Weng W, Tu J (2018). A Numerical Study on Firefighter
 760 Nasal Airway Dosimetry of Smoke Particles from a Realistic Composite
 761 Deck Fire. *Journal of Aerosol Science*, 123: 91–104.

762 Yang L, Ye M (2014). CFD Simulation Research on Residential Indoor Air
 763 Quality. *Science of the Total Environment*, 472: 1137–44.

764 You S, Yao Z, Dai Y, Wang CH (2017). A Comparison of PM Exposure Related
 765 to Emission Hotspots in a Hot and Humid Urban Environment:
 766 Concentrations, Compositions, Respiratory Deposition, and Potential
 767 Health Risks. *Science of the Total Environment*,.
 768 <https://doi.org/10.1016/j.scitotenv.2017.04.217>.

769 Zhang Z, Chen X, Mazumdar S, Zhang T, Chen Q (2009). Experimental and
 770 Numerical Investigation of Airflow and Contaminant Transport in an
 771 Airliner Cabin Mockup. *Building and Environment*,.
 772 <https://doi.org/10.1016/j.buildenv.2008.01.012>.

773 Zhao B, Chen C, Tan Z (2009). Modeling of Ultrafine Particle Dispersion in
 774 Indoor Environments with an Improved Drift Flux Model. *Journal of*
 775 *Aerosol Science*, 40(1): 29–43.

776

777 **Acknowledgements:**

778We thank the Indoor Environment Group of Lawrence Berkeley National Laboratory
779for providing the measured indoor and outdoor air quality data. This study was
780supported by National Key R&D Program of China (Grant No. 2016YFC0802801 and
7812016YFC0802807), National Science Fund for Distinguished Young Scholars of China
782(Grant No 71725006), National Natural Science Foundation of China (Grant No.
78351706123). This work was also supported by the Office of Energy Efficiency and
784Renewable Energy, the United States Department of Energy under Contract No. DE-
785AC02-05CH11231. The authors are deeply grateful to these supports.

786

787

788**Author contributions:**

789N.L., W.W. and T.H. designed the study. N.L., X.X. and K.S. conducted the combined
790simulation of the OB-based indoor environment. All authors participated in writing
791and revising the manuscript. All authors read and approved the submitted
792manuscript.